Total chemical synthesis and electrophysiological characterization of mechanosensitive channels from *Escherichia coli* and *Mycobacterium tuberculosis*

Daniel Clayton*, George Shapovalov†, Joshua A. Maurer‡, Dennis A. Dougherty‡, Henry A. Lester†, and Gerd G. Kochendoerfer*§

*Gryphon Therapeutics, 600 Gateway Boulevard, South San Francisco, CA 94080; and Divisions of ‡Chemistry and Chemical Engineering and †Biology, California Institute of Technology, Pasadena, CA 91125

Total chemical protein synthesis was used to generate multimilligram quantities of the mechanosensitive channel of large conductance from *Escherichia coli* (Ec-MscL) and *Mycobacterium tuberculosis* (Tb-MscL). Cysteine residues introduced to allow chemical ligation were masked with cysteine-reactive molecules, resulting in side chain functional groups similar to those of the wild-type protein. Synthetic channel proteins were transferred to 2,2,2-trifluoroethanol and reconstituted into vesicle membranes. Fluorescent imaging of vesicles showed that channel proteins were membrane-localized. Single-channel recordings showed that reconstituted synthetic Ec-MscL has conductance, pressure dependence, and substate distribution similar to those of the recombinant channel. Reconstituted synthetic Tb-MscL also displayed conductance and pressure dependence similar to that of the recombinant protein. Possibilities for the incorporation of unnatural amino acids and biophysical probes, and applications of such synthetic ion channel analogs, are discussed.

R ecently, ion channel research has been aided by the discovery of bacterial ion channels that share many key features of mammalian channels (1–3). Some of these bacterial channel proteins are smaller and more amenable to expression and purification than mammalian channels. Importantly, bacterial channels can often be reconstituted into vesicles and other synthetic membrane systems, allowing detailed functional characterization (4–6). Furthermore, several bacterial channels have been described at atomic resolution by x-ray crystallography (7–11), providing opportunities for correlating structure and function in a key class of membrane protein.

Although the preparation of many medium-sized water-soluble proteins by chemical ligation is now a routine procedure (12–14), the synthesis of ion channels and other membrane proteins presents unique challenges. Many hydrophobic peptides have sequences that couple inefficiently, meaning that the synthesis of each segment must be optimized. Hydrophobic peptides also have limited solubility and tend to aggregate. Furthermore, after synthesis is complete the native oligomeric protein must be formed from unfolded monomers. However, recent advances in chemical ligation methodologies have permitted the semisynthesis (15) and the total chemical synthesis of membrane proteins, including the 97-residue type III (single membrane-spanning segment) M2 protein of the influenza virus (16). The synthetic M2 protein assembled into the native tetrameric form on reconstitution into dodecylphosphocholine micelles.

Here, we describe the chemical synthesis of two polytopic membrane proteins, the mechanosensitive ion channels from *Escherichia coli* (Ec-MscL) and *Mycobacterium tuberculosis* (Tb-MscL), and the vesicle reconstitution of these channels into a form functionally similar to that of the recombinant protein. Multimilligram quantities of Ec-MscL and Tb-MscL were generated by optimizing synthesis, purification, and ligation proto-cols previously developed for producing hydrophobic membrane proteins, thus allowing vesicle reconstitution, and then patch-clamp analysis. The ability to synthesize, reconstitute, and functionally characterize ion channels presents new possibilities for ion channel research. Unnatural amino acids and fluorescent or EPR spin-labels can now be incorporated site-specifically, allowing a variety of detailed investigations into channel function. Also, ion channels are sensitive chemical sensors, producing detectable signals from single-molecule events. Therefore, synthetic channels could allow the development of novel biosensors or bioelectronic materials.

Materials and Methods

Peptide Synthesis and RP-HPLC Purification. Peptide segments were synthesized on either a thioester-generating resin (17) or a (–O–CH2)–phenylacetamidomethyl resin by using standard *tert*-butoxycarbonyl chemistry with *in situ* neutralization (18), then cleaved and deprotected with hydrogen fluoride at 0°C in the presence of *p*-cresol. Acetamidomethyl (Acm) was used as a nonstandard side chain protecting group for cysteine residues to inhibit self-ligation during segment assembly, and the N-terminal segment was biotinylated on-resin by using a 10-fold molar excess of NHS-biotin (Novabiochem) in anhydrous DMSO (Sigma-Aldrich). Target peptides were solubilized with mixtures of water and 2,2,2-trifluoroethanol (TFE) (Sigma-Aldrich) and purified by preparative RP-HPLC on a Rainin Instruments Dynamax system with a 2.2 (i.d.) × 25-cm (10-μm particle size) Vydac (Hesperia, CA) C4 column. Electrospray ionization (ESI)-MS was performed on either a PE Sciex (Thornhill, ON, Canada) API-III triple quadrapole or an API-150 single quadrapole mass spectrometer to identify the target peptides. Theoretical peptide masses (average isotope composition) were calculated by MACPROMASS (T. Lee, City of Hope, Duarte, CA), and experimental masses were calculated by reconstruction from ESI-MS data in MACSPEC (PE Sciex) or ANALYST (MDS Sciex, Concord, ON, Canada). Peptide purity was assessed on a 0.46 (i.d.) × 15-cm Vydac C4 column (5-μm particle size), using a Hewlett–Packard 1100 quaternary pump high-pressure mixing system (see *Supporting Materials and Methods*, which is published as supporting information on the PNAS web site, for more detail on experimental procedures).

Chemical Protein Synthesis, Purification, and Transfer to TFE. Ligations were performed with peptide concentrations of 0.1 mM in

---

48 mM dodecylphosphocholine (DPC) (Avanti Polar Lipids) and 8 M urea in 250 mM phosphate buffer (pH 7.5) at 40°C. Reactions were initiated by the addition of 0.5% thiophenol (Fluka) and monitored by analytical RP-HPLC and ESI-MS analysis. Ligated product was treated with a 5-fold excess (vol/vol) of 20% 2-mercaptoethanol (Fluka) in 48 mM DPC/8 M urea solution (pH 5) at 40°C for 5 min, then with Tris-carboxyethyl phosphine (TCEP) (Fluka Chemicals) for a further 3 min. The product from the first ligation was purified by preparative C4 RP-HPLC over 20 min on a 35–65% gradient of buffer C [6:3:1, isopropanol:acetonitrile:water with 0.1% trifluoroacetic acid (Halocarbon, River Edge, NJ)]. The Acm protecting group on the N-terminal cysteine residue was removed from this product by reaction for 45 min with a 15-fold molar excess of Hg(II) acetate (Fluka). 2-mercaptoethanol was added to this solution to a concentration of 2% (vol/vol) and reacted for 15 min to scavenge Hg^{2+}, and then TCEP was added. Deprotected product was purified on a 45–65% gradient of buffer C over 5 min, and the material was pooled and lyophilized. Product from the second and final ligation was purified on a 55–75% gradient over 15 min, and the sulfhydryl groups were modified at room temperature (pH 7.5) with a 30-fold molar excess of bromoacetamide (Sigma-Aldrich). Full-length biotinylated, cysteine-modified Ec-MscL(1–136) was then purified on a 60–80% gradient of buffer C over 25 min. Similar methods of chemical synthesis and purification were used to produce synthetic Tb-MscL.

Pure synthetic Ec-MscL and Tb-MscL were transferred from HPLC buffers to TFE by addition of 5 vol of freshly distilled TFE to the HPLC pool, adjustment of the pH to 7 with ammonia, and sample volume reduction, by evaporation under vacuum, to give a final product concentration of 2 mg/ml (see *Supporting Materials and Methods* for more detail on experimental procedures).

Vesicle Reconstitution of Synthetic and Recombinant Ec-MscL. Fifty microliters of a 10 mg/ml solution of azolectin (Sigma-Aldrich) in chloroform was air-dried on Teflon for 15 min, redissolved with 5 μl of a 2 mg/ml solution of synthetic channel protein in TFE (19), and allowed to dry for 15 min. The resultant film of material was desiccated under house vacuum for 1 h and then rehydrated for 1 h with 5 μl of 250 mM KCl/5 mM Hepes/0.1 mM EDTA (20). One microliter of this rehydrated lipid was applied to the glass coverslip of the recording chamber and allowed to air dry for 10 min, and 0.5 μl of 1 M $MgCl_2$ was spread on the coverslip and dried for 10 min. Three hundred microliters of rehydration buffer was then added to the recording chamber, and blister formation was allowed to proceed for 30 min. Control samples were prepared in a similar manner. These vesicle preparations were the starting point for both fluorescence and patch-clamp experiments. After transfer to TFE, WT recombinant Tb-MscL was also vesicle-reconstituted for electrophysiological measurements (see *Supporting Materials and Methods* for more detail on experimental procedures).

Fluorescence Imaging. Two microliters of a 0.1 mg/ml solution of streptavidin-Alexa Fluor 488 conjugate (Molecular Probes) in PBS was added to vesicle preparations containing reconstituted synthetic Ec-MscL or Tb-MscL, or lacking channel protein. Vesicles were observed during 1 h on an Olympus IX71 inverted microscope equipped with a shuttered 175-W xenon arc lamp, a 488-nm excitation filter, a 515-nm fluorescence cube, and an Olympus Plan Apo 60×/1.4 numerical aperture (N.A.) oil immersion objective. Images were captured on a Photometrix (San Diego) Cascade charge-coupled device camera. Exposure times were 100 ms for brightfield images and 200–300 ms for fluorescence images.

Electrophysiological Characterization. Single-channel recordings were made at 20–22°C on synthetic Ec-MscL and Tb-MscL, and on recombinant Ec-MscL at a bandwidth of 20 kHz at 50 mV (intracellular medium is negative) in symmetrical 250 mM KCl/1 mM $MgCl_2$/5 mM Hepes (pH 7.1) solution. Currents were acquired with an Axopatch 200B amplifier, a Digidata 1322A digitizer, and PCLAMP 8 software (all from Axon Instruments, Union City, CA). The probability of opening (P_{open}) vs. suction curves were generated by software designed by one of the authors (G.S.). Boltzmann distributions were fitted to the dose–response relations by using ORIGIN 6.0 software (Microcal, Northampton, MA), yielding activation midpoints and gradients. The curves on the all-points histograms were normalized to match the areas under the peaks corresponding to fully open states of synthetic and recombinant Ec-MscL.

Results

Synthetic Strategy. The general strategy used for the total chemical synthesis of Ec-MscL is shown in Fig. 1. A challenge for the chemical synthesis of Ec-MscL and Tb-MscL was the absence of cysteine residues in the WT sequence (21, 22); introduction of cysteine residues at ligation sites results in the presence of nonnative sulfhydryl groups in the final protein. For the synthesis of Ec-MscL, glutamine 56 (Q56) and asparagine 103 (N103) were changed to cysteine, based on unpublished data (J.A.M.) indicating that these side chains are not critical to channel function. To minimize contributions from nonnative groups in the target sequence, the full-length protein was reacted with bromoacetamide (23), which selectively modifies the two introduced cysteine residues and produces side chain functional groups that are sterically and electronically similar to those of the WT residues. For the synthesis of Tb-MscL, glutamate 102 (E102) and serine 52 (S52) (22) were changed to cysteine and then masked in the final product with appropriate cysteine-reactive molecules (Fig. 5, which is published as supporting information on the PNAS web site). Both synthetic strategies also incorporated an N-terminal biotin moiety during segment synthesis to aid in fluorescent labeling.

Multimilligram Quantities of Channel Protein Were Generated by Using an Optimized Synthesis Procedure. A particular concern in the total chemical synthesis of membrane proteins is the difficulty in preparing and handling the hydrophobic peptide segments. However, by using an optimized *in situ* peptide synthesis protocol and including a TFE solubilization step into the purification procedure to overcome the limited solubility of the peptide segments, we achieved final yields of 25–30% for Ec-MscL(56–102) and Ec-MscL(103–136), and 15% for Ec-MscL(1–55). Yields of 15–30% were also observed for the Tb-MscL segments. Target peptides were ≈95% pure by analytical RP-HPLC analysis. Experimental masses of the segments were within 1 Da of the theoretical mass. For Ec-MscL segments, masses were as follows: MscL(1–55)-α-thioester, experimental mass = 6,217.5 ($\pm$1) (theoretical mass = 6,218.1 Da); MscL(56–102)-α-thioester, experimental mass = 5,698.5 ($\pm$1) (theoretical mass = 5,698.4 Da); and MscL(103–136)-carboxylate, experimental mass = 3,217.5 ($\pm$1) (theoretical mass = 3,218.1Da).

The limited solubility of the peptide segments in ligation buffers was overcome by the use of increased temperature (40°C), high denaturant concentration (8 M urea), and the addition of DPC to ligation reactions. Pure ligated product was obtained by using isopropanol-containing buffer gradients similar to those used for peptide segment purification. Subsequent treatment of the HPLC pool of pure material with an excess of Hg(II) acetate for 45 min resulted in the quantitative removal of the Acm protecting group from the N-terminal cysteine residue. Purification of this deprotected product, Ec-MscL(56–136), after 2-mercaptoethanol and TCEP treatment resulted in ma-
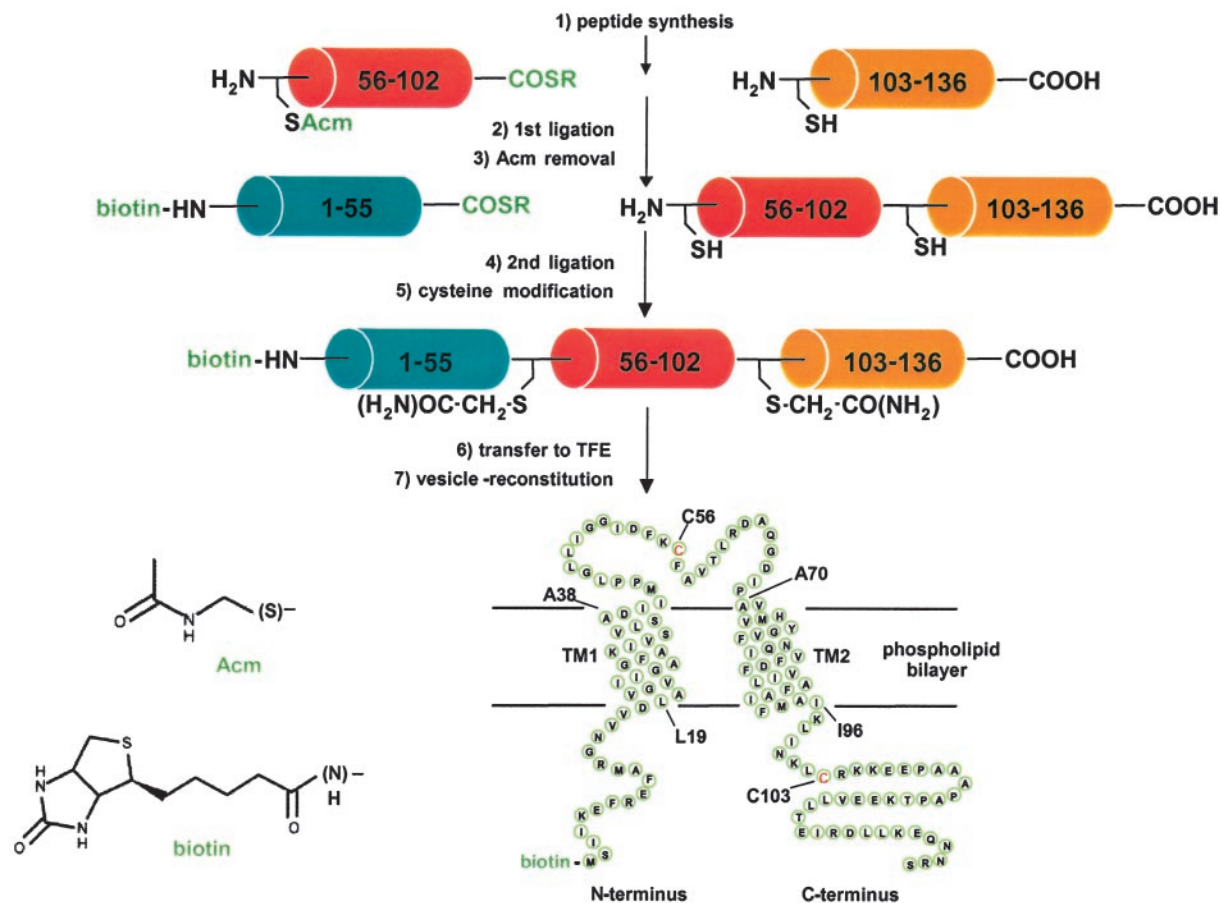
Fig. 1. Strategy for the total chemical synthesis of Ec-MscL. The major steps of the synthesis are listed numerically. Peptide sequences are as follows: (biotin)-MscL(1–55)-α-thioester, MSIIKEFRE FAMRGNVVDLAVGVIIGAAFGKIVSSLVADIIMPPLGLLIG GIDFK; MscL(56–102)-α-thioester (Q56C), FAVTLRDAQG-DIPAVVMHYGVFIQNVF DFLIVAFAIFMAIKLI NKL; MscL(103–136)-carboxylate (N103C), RKKEEPAAAPAP TKEEVLLTEIRDLLKEQNNRS. The Acm cysteine protecting group, the biotin moiety, and the C-terminal α-thioester group (COSR; R, auxiliary amino acid) are shown in green. The structures of the N-terminal modifying groups are shown in the lower left of the figure, and the expected topology of the channel protein in the phospholipid bilayer is shown at the lower right of the figure. Relevant amino acids are indicated on this topological map to define the limits of the probable transmembrane helices (TM1, L19-A38; TM2, A70-I96), as listed on the Swiss-Prot database (http://us.expasy.org; entry P23867), and the ligation sites (cysteine residues), which are also shown in red.

terial [experimental mass = 9,138.5 (±1.5) (theoretical mass = 9,137.8 Da)] of ≥95% purity as assessed by analytical RP-HPLC.

Similar buffer conditions also efficiently solubilized reactant peptides in the final ligation reactions, and comparable purification protocols yielded pure ligated product. Attempts at modifying cysteine residues with bromoacetamide directly in the HPLC pool resulted in very slow and incomplete reactions. Quantitative modification of cysteine residues was achieved by performing this reaction after a 4-fold concentration of the pool by lyophilization in the presence of DPC. Purification yielded correctly modified product [Ec-MscL, experimental mass = 15,266.5 (±2) (theoretical mass = 15,265.8 Da); Tb-MscL, experimental mass = 16,301.5 (±2) (theoretical mass = 16,300.7 Da)], and RP-HPLC analysis of synthetic Ec-MscL (Fig. 2) and Tb-MscL (Fig. 6, which is published as supporting information on the PNAS web site) showed that the final product was ≥95% pure. Yields of between 20% and 50% were achieved for purification of ligated and modified Ec-MscL and Tb-MscL segments. Final yields of pure, modified full-length protein for both Ec-MscL and Tb-MscL were ≈4 mg.

Transfer of the synthetic channel to an organic solvent able to dissolve dialkylphospholipid was a necessary step for vesicle reconstitution. Initial attempts to transfer synthetic protein to TFE resulted in only partial solubilization (≈0.5 mg/ml). When the volume of TFE added to the HPLC pool was increased and

the pH was adjusted before and during transfer, clear solutions of synthetic Ec-MscL and Tb-MscL (2 mg/ml) were obtained. RP-HPLC and ESI-MS analysis of these TFE solutions showed that modifications had not occurred during buffer transfer.

Vesicle Formation in the Recording Chamber Reliably Produces Blisters. Vesicle reconstitution was performed to fold synthetic Ec-MscL and Tb-MscL into their native conformation, in a lipid bilayer system amenable to fluorescence and electrophysiology experiments. The first step of this process involved forming an azolectin film on a Teflon slide, then redissolving this film with an aliquot of synthetic channel in TFE. This resulted in a layer of lipid and protein on the Teflon having the desired molar ratio (≈1,000:1). After desiccation and rehydration of this film, high concentrations of multilamellar vesicles were observed by light microscopy. However, very few blisters developed when aliquots of this vesicle preparation were transferred to a recording chamber with Mg²⁺-containing solution. Large increases in the number of blisters were achieved by applying an aliquot of the lipid preparation and of concentrated MgCl₂ solution directly to the recording chamber, then drying and rehydrating the resultant film. Furthermore, vesicles in these preparations adhered to the bottom of the recording chamber, simplifying the search for blisters suitable for subsequent patch-clamp experiments.
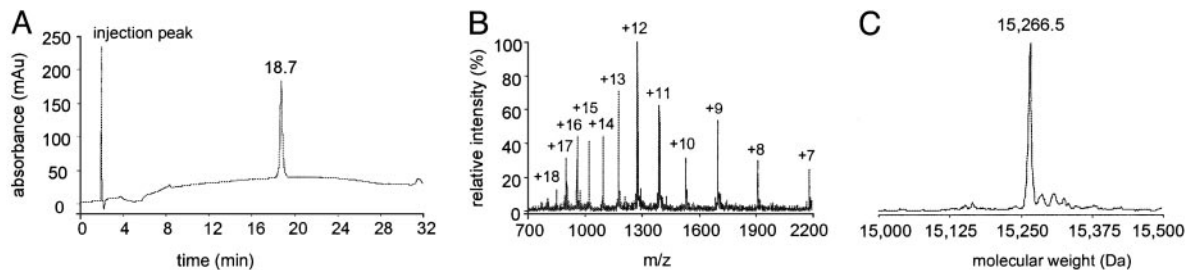
Fig. 2. RP-HPLC and ESI-MS analysis of synthetic Ec-MscL. (*A*) Analytical RP-HPLC chromatogram (25–100% buffer C, 26 min) for the final product. (*B*) ESI mass spectrum with the observed charge states labeled. (*C*) Mass reconstruct from the charged states (minor peaks in the ESI-MS reconstruct showing masses slightly greater than the target peptide are Na⁺ adducts).

Ec-MscL and Tb-MscL Are Membrane-Localized After Vesicle Reconstitution. The N-terminal biotin moieties of Ec-MscL and Tb-MscL were modified with streptavidin-Alexa Fluor 488 to allow fluorescence imaging. Brightfield and fluorescence images of vesicle preparations generated in the presence and the absence of synthetic Ec-MscL are shown in Fig. 3. Fluorescence images of vesicles prepared in the presence of channel protein clearly show strong fluorescence localized to the membrane portion, weaker and more disperse fluorescence in the lumen of the vesicle, and little or none in solution (Fig. 3 *B* and *D*). This membrane-localized fluorescence was first observed 10 min after the addition of fluorescent label, and increased in intensity over 1 h. After 1 h, all of the vesicles located by brightfield microscopy and then viewed in the focal plane also showed membrane-localized fluorescence. In contrast, the control sample showed only diffuse fluorescence in the solution and no membrane-localized fluorescence even several hours after the addition of

the fluorescent label (Fig. 3*F*). Fluorescence experiments on vesicle-reconstituted Tb-MscL show similar results (Fig. 7, which is published as supporting information on the PNAS web site). The results of these fluorescence experiments demonstrate that synthetic Ec-MscL and Tb-MscL have associated with the vesicle membrane during the reconstitution procedure.

Tension-Gated Single-Channel Activity in Vesicle-Reconstituted Synthetic Ec-MscL. Patch-clamp experiments were performed to assess correct folding of vesicle-reconstituted synthetic Ec-MscL. The vesicle preparations yielded patches with resistances of 5–20 GΩ. Single-channel activity was recorded and analyzed from >20 patches. Suction produced characteristic single-channel activity. Brief (<10 ms) partial and full channel openings were first observed at a suction of ≈0.7 psi (1 psi = 6.89 kPa), whereas sustained channel openings were observed at ≈0.9 psi (Fig. 4*A*). In some patches, multiple superimposed openings were observed
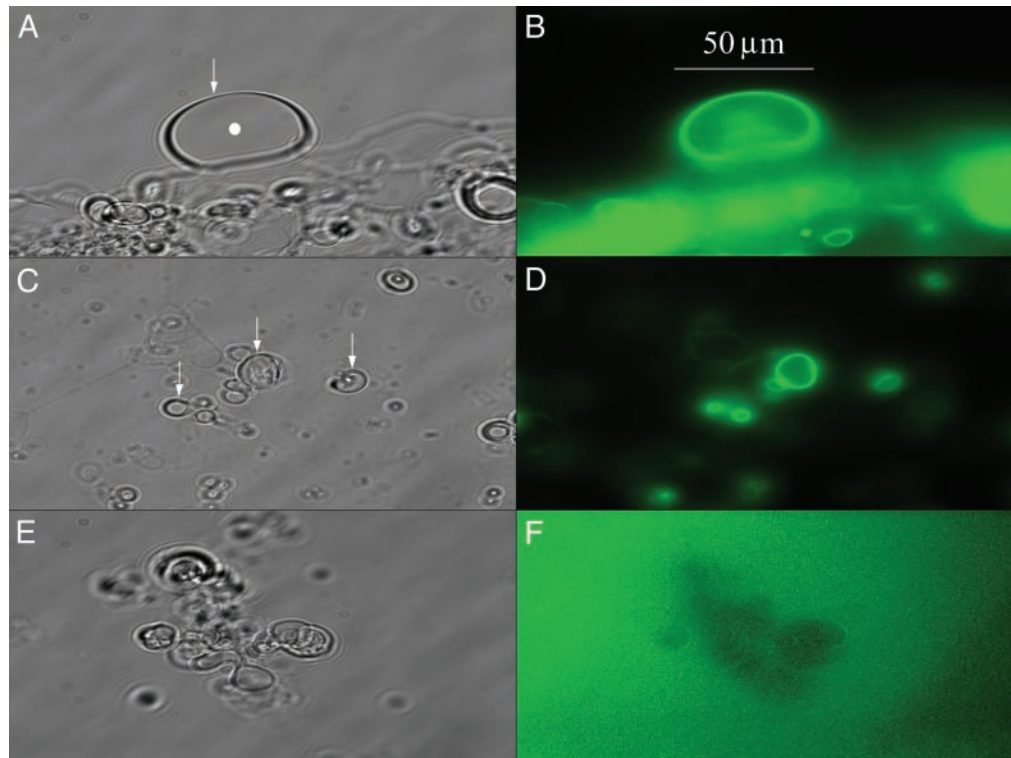

Fig. 3. Fluorescence imaging of vesicle-reconstituted synthetic Ec-MscL. *A* and *C* show brightfield images of vesicles generated in the presence of synthetic Ec-MscL, and *B* and *D* show the corresponding fluorescence images. Several vesicles or groups of vesicles are indicated by arrows in *A* and *C*, and the lumen of the large vesicle in *A* is indicated by a filled circle. The arrow in *A* also indicates the vesicle membrane. Vesicles in these preparations are attached to the bottom of the recording chamber. *E* and *F* show the brightfield and corresponding fluorescence image of vesicles generated in the absence of synthetic Ec-MscL. Regions of diffuse fluorescence observed in *B* and *D* result from vesicles not in the focal plane.
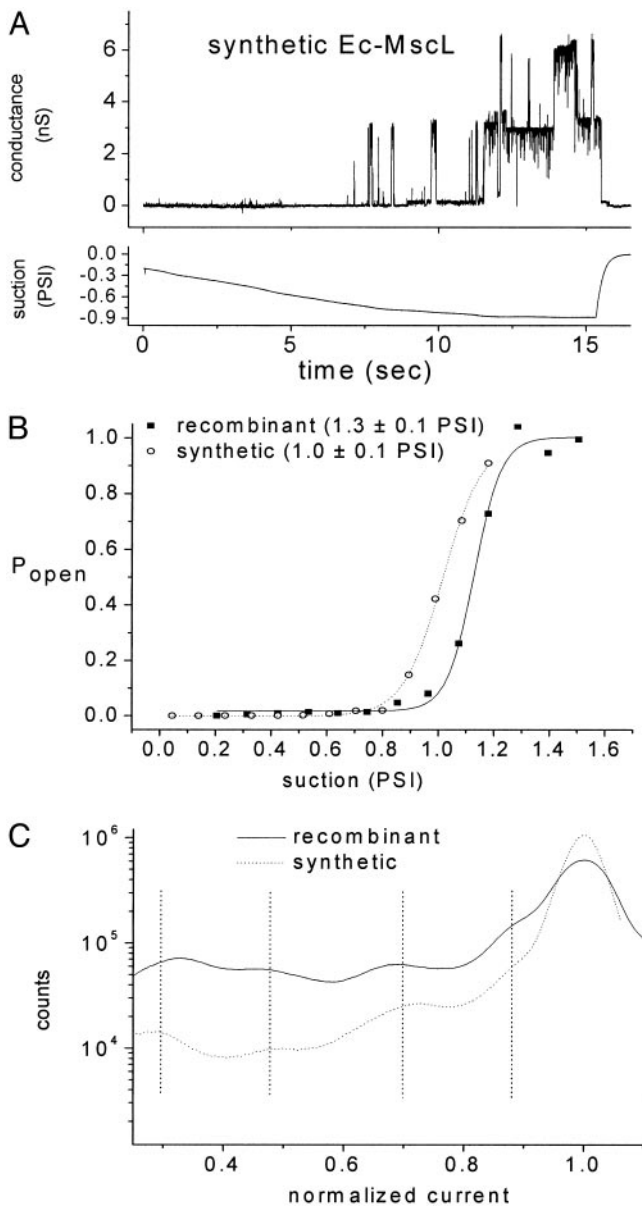
BIOCHEMISTRY

Fig. 4. Electrophysiological analysis of vesicle-reconstituted Ec-MscL. (*A*) A sample trace of synthetic Ec-MscL activity (upper trace) during a ramp of applied suction (lower trace). (*B*) Dose–response (suction–P_{open}) relations for synthetic (open circles) and recombinant (filled squares) Ec-MscL. Also shown in *B* are the average midpoint values and standard errors calculated from the 6 and 10 P_{open} vs. suction curves, respectively. (*C*) All-points histograms for synthetic and recombinant Ec-MscL generated from five and eight conductance traces, respectively. Dashed vertical lines on *C* emphasize the similar conductance substates of synthetic and recombinant Ec-MscL.

at higher suction (Fig. 4*A*). When suction was released, all channel activity disappeared. No corresponding conductance was observed when suction was applied to patches formed from vesicles produced in the absence of channel protein. In general, the electrophysiological features of synthetic Ec-MscL activity closely resemble those observed for recombinant Ec-MscL (24–26): open-channel conductance of 3 nS; the presence of multiple substates; and the overall sensitivity to suction (24–26).

Synthetic and WT Ec-MscL Have Similar Activation Thresholds and Comparable Substate Conductances. Probability of opening (P_{open}) vs. suction curves and all-points histograms allowed more de-

tailed kinetic comparison of synthetic and recombinant Ec-MscL. For these analyses, conductance recordings were made on multiple-channel patches while a ramp of suction was applied. Dose–response (suction–P_{open}) relationships for recombinant (solid squares) and synthetic (open circles) Ec-MscL are shown in Fig. 4*B*. The average midpoints ($\pm$SEM) of these curves are $x_o = 1.0 \pm 0.1$ psi (7 $\pm$ 1 kPa, 6 traces) for synthetic and 1.3 $\pm$ 0.1 psi (9 $\pm$ 1 kPa, 10 traces) for recombinant Ec-MscL. The small difference in midpoints does not, in our judgment, reveal a significant difference in the suction sensitivity of synthetic Ec-MscL vs. recombinant Ec-MscL. Also, the similar average gradient at the midpoint of the dose–response curves ($\delta = 0.06 \pm 0.01$ psi for both synthetic and recombinant channel) shows equal suction dependence on gating. The ratio δ/x_o is 0.05 for recombinant Ec-MscL and 0.06 for synthetic Ec-Mscl, in agreement with the value of 0.05 ($\pm$0.01 for all ratios) reported previously (25). The all-points histograms generated from traces containing either 1 or 2 channels (eight traces for recombinant and five traces for synthetic Ec-MscL) are shown in Fig. 4*C*. These data show that both synthetic and recombinant Ec-MscL occupy conductance substates for <5% of the time spent in the highest-conductance open state. The all-points histograms were fitted to multiple Gaussian components to reveal substate conductances; these substate conductances were equal for the synthetic and recombinant channels (vertical lines in Fig. 4*C*), suggesting that the structural trajectory of channel opening is similar for both synthetic and recombinant Ec-MscL.

The Increased Pressure Response of Synthetic Tb-MscL Mimics That of Recombinant Tb-MscL. Electrophysiological studies were also performed on vesicle-reconstituted synthetic Tb-MscL. Single-channel openings (five traces acquired, one shown in Fig 8, which is published as supporting information on the PNAS web site) showed typical mechanosensitive single-channel activity, with conductance similar to that of synthetic Ec-MscL (3 nS) and recombinant Tb-MscL (5). As with recombinant Tb-MscL (5, 6), $\approx$2-fold greater suction (2 psi) was needed to achieve channel opening of synthetic Tb-MscL, as compared to synthetic or recombinant Ec-MscL. In most traces, channel openings of synthetic Tb-MscL were followed by membrane rupture (maximum observed P_{open} was <0.1), and so it was not possible to perform detailed analyses similar to those described previously for Ec-MscL. However, to the extent that such characterization was possible, synthetic Tb-MscL is functionally similar to recombinant Tb-MscL.

Discussion

Chemical protein synthesis has provided multimilligram quantities of unfolded synthetic biotinylated Ec-MscL and Tb-MscL for vesicle reconstitution and electrophysiological characterization. Cysteine residues required for chemical ligation were masked by modification with cysteine-reactive compounds, resulting in side chain functional groups similar to those of the WT protein (23). Subsequent electrophysiological characterization showed that the small differences in the side chain length of these residues did not affect channel function. A robust and reproducible protocol for producing a biotinylated version of synthetic Ec-MscL and Tb-MscL was developed by making key improvements to current protocols, such as the addition of organic solvent and detergent during purification and ligation, and by performing the deprotection and modification of cysteine residues without full lyophilization and redissolution. This optimized synthesis protocol appears generally applicable because Ec-MscL, Tb-MscL, and several fluorescently labeled analogs of Ec-MscL (data not shown) were successfully made.

Synthetic Ec-MscL and Tb-MscL were reconstituted into vesicles. Key features of the protocol are the transfer of the channel protein from RP-HPLC buffers to TFE by evaporative

Clayton *et al.*

solvent exchange; the redissolution of a dry azolectin film with this TFE solution containing channel protein; and the final rehydration of vesicles and divalent cation-induced blister formation in the recording chamber. The incorporation of the N-terminal biotin moiety during segment synthesis allowed a fluorescent label to be used to establish membrane-localization of Ec-MscL and Tb-MscL.

Vesicle preparations generated directly in the electrophysiological recording chamber contained numerous blisters suitable for producing GΩ seals in patch-clamp experiments. Furthermore, the level of mechanosensitive ion channel activity found in excised patches indicated that the reconstitution protocol is highly efficient. Recordings from excised patches containing either synthetic or recombinant Ec-MscL, and the subsequent analyses, indicate that synthetic Ec-MscL is functionally the same as recombinant Ec-MscL: the single-channel conductance (3 nS) is similar for both channels; similar conductance substates are present; and there is little or no difference in their suction sensitivity. The conductance and gating characteristics of synthetic Tb-MscL mimicked those of recombinant Tb-MscL. The functional similarities observed between synthetic and recombinant channels demonstrate that they have folded to their native oligomeric structures.

The ability to synthesize, reconstitute, and electrophysiologically characterize ion channels provides many new possibilities for further investigation. A wide range of chemical modifications can now be introduced with the precise control that total chemical synthesis allows (23, 27–28). For example, fluorescent unnatural amino acids can be introduced (29–31), allowing a more direct, and so more quantitative, fluorescence-imaging approach than the biotin-streptavidin Alexa Fluor 488 protocol used here. Fluorescently labeled analogs will allow a variety of fluorescence resonance energy transfer (FRET) studies to be performed, and may also allow the simultaneous recording of single-channel conductance and single-molecule FRET. We anticipate that the present synthesis and vesicle-reconstitution protocols will be broadly applicable to studies on diverse ion channels.

1. Jan, L. Y. & Jan, Y. N. (1997) *Annu. Rev. Neurosci.* **20,** 91–123.
2. Connolly, D. L., Shanahan, C. M. & Weissberg, P. L. (1998) *Int. J. Biochem. Cell Biol.* **30,** 169–172.
3. Martinac, B. & Kloda, A. (2003) *Prog. Biophys. Mol. Biol.* **82,** 11–24.
4. Hase, C. C., Le Dain, A. C. & Martinac, B. (1995) *J. Biol. Chem.* **270,** 18329–18334.
5. Moe, P. C., Levin, G. & Blount, P. (2000) *J. Biol. Chem.* **275,** 31121–31127.
6. Shapovalov, G., Bass, R., Rees, D. C. & Lester, H. A. (2003) *Biophys. J.* **84,** 2357–2365.
7. Doyle, D. A., Morais Cabral, J., Pfuetzner, R. A., Kuo, A., Gulbis, J. M., Cohen, S. L., Chait, B. T. & MacKinnon, R. (1998) *Science* **280,** 69–77.
8. Chang, G., Spencer, R. H., Lee, A. T., Barclay, M. T. & Rees, D. C. (1998) *Science* **282,** 2220–2226.
9. Fu, D., Libson, A., Miercke, L. J., Weitzman, C., Nollert, P., Krucinski, J. & Stroud, R. M. (2000) *Science* **290,** 481–486.
10. Bass, R. B., Strop, P., Barclay, M. & Rees, D. C. (2002) *Science* **298,** 1582–1587.
11. Jiang, Y., Lee, A., Chen, J., Ruta, V., Cadene, M., Chait, B. T. & MacKinnon, R. (2003) *Nature* **423,** 33–41.
12. Wilken, J. & Kent, S. B. (1998) *Curr. Opin. Biotechnol.* **9,** 412–426.
13. Dawson, P. E. & Kent, S. B. (2000) *Annu. Rev. Biochem.* **69,** 923–960.
14. Kochendoerfer, G. G. (2001) *Curr. Opin. Drug Discovery Dev.* **4,** 205–214.
15. Valiyaveetil, F. I., MacKinnon, R. & Muir, T. W. (2002) *J. Am. Chem. Soc.* **124,** 9113–9120.
16. Kochendoerfer, G. G., Salom, D., Lear, J. D., Wilk-Orescan, R., Kent, S. B. & DeGrado, W. F. (1999) *Biochemistry* **38,** 11905–11913.
17. Camarero, J. & Muir, T. W. (1995) in *Current Protocols in Protein Science*, eds. Coligan, J. E., Dunn, B. M., Ploegh, H. L., Speicher, D. W. & Wingfield, P. T. (Wiley, New York), pp. 18.4.1–18.4.21.
18. Schnölzer, M., Alewood, P., Jones, A., Alewood, D. & Kent, S. B. (1992) *Int. J. Pept. Protein Res.* **40,** 180–193.
19. Lougheed, T., Borisenko, V., Hand, C. E. & Woolley, G. A. (2001) *Bioconjugate Chem.* **12,** 594–602.
20. Delcour, A. H., Martinac, B., Adler, J. & Kung, C. (1989) *Biophys. J.* **56,** 631–636.
21. Sukharev, S. I., Blount, P., Martinac, B., Blattner, F. R. & Kung, C. (1994) *Nature* **368,** 265–268.
22. Cole, S. T., Brosch, R., Parkhill, J., Garnier, T., Churcher, C., Harris, D., Gordon, S. V., Eiglmeier, K., Gas, S., Barry, C. E., III, *et al.* (1998) *Nature* **393,** 537–544.
23. Kochendoerfer, G. G., Chen, S. Y., Mao, F., Cressman, S., Traviglia, S., Shao, H., Hunter, C. L., Low, D. W., Cagle, E. N., Carnevali, M., *et al.* (2003) *Science* **299,** 884–887.
24. Sukharev, S. I., Blount, P., Martinac, B. & Kung, C. (1997) *Annu. Rev. Physiol.* **59,** 633–657.
25. Sukharev, S. I., Sigurdson, W. J., Kung, C. & Sachs, F. (1999) *J. Gen. Physiol.* **113,** 525–540.
26. Anishkin, A., Gendel, V., Sharifi, N. A., Chiang, C. S., Shirinian, L., Guy, H. R. & Sukharev, S. (2003) *J. Gen. Physiol.* **121,** 227–244.
27. Wilken, J., Hoover, D., Thompson, D. A., Barlow, P. N., McSparron, H., Picard, L., Wlodawer, A., Lubkowski, J. & Kent, S. B. (1999) *Chem. Biol.* **6,** 43–51.
28. Huse, M., Holford, M. N., Kuriyan, J. & Muir, T. W. (2000) *J. Am. Chem. Soc.* **122,** 8337–8338.
29. Sydor, J. R., Herrmann, C., Kent, S. B., Goody, R. S. & Engelhard, M. (1999) *Proc. Natl. Acad. Sci. USA* **96,** 7865–7870.
30. Cotton, G. J. & Muir, T. W. (2000) *Chem. Biol.* **7,** 253–261.
31. Becker, C. F., Hunter, C. L., Seidel, R., Kent, S. B., Goody, R. S. & Engelhard, M. (2003) *Proc. Natl. Acad. Sci. USA* **100,** 5075–5080.

BIOCHEMISTRY